Modeling Stiffness and Damping in Rotational Degrees of Freedom Using Multibond Graphs

Georges Tod, François Malburet, Julien Gomand, Pierre-Jean Barre
Arts et Metiers Paristech, CNRS, LSIS
13617 Aix-en-Provence, France
georges.tod@ensam.eu, francois.malburet@ensam.eu, julien.gomand@ensam.eu

***Abstract*— a contribution is proposed for the modeling of mechanical systems using multibond graphs. When modeling a physical system, it may be needed to catch the dynamic behavior contribution of the joints between bodies of the system and therefore to characterize the stiffness and damping of the links between them. The visibility of where dissipative or capacitive elements need to be implemented to represent stiffness and damping in multibond graphs is not obvious and will be explained. A multibond graph architecture is then proposed to add stiffness and damping in three rotational degrees of freedom. The resulting joint combines the spherical joint multibond graph relaxed causal constraints while physically representing three concatenated revolute joints. The mathematical foundations are presented, and then illustrated through the modeling and simulation of an inertial navigation system; in which stiffness and damping between the gimbals are taken into account. This method is particularly useful when modeling and simulating multibody systems using Newton-Euler formalism in multibond graphs. Future work will show how this method can be extended to more complex systems such as rotorcraft blades' connections with its rotor hub.**

Keywords—multibody dynamics; multibond graphs; spherical joint; revolute joint; causality

NOMENCLATURE

$\underline{\omega_{a,b}^{c}}$	Angular velocity vector between bodies a and b expressed in body c reference frame
$\underline{v}$	Vector
$\underline{0}$	Null vector
R_j	Reference frame attached to body j
$M_{j\to j+1}$	Rotation matrix between bodies j and j+1
MBG	Multibond graph

Multibond graph power arrows transport a three dimensional flow vector and a three dimensional effort vector.

I. INTRODUCTION

In order to analyze the dynamics of a mechanical system, an intermediate step can be to model the system with a multibody approach. In order to obtain a mathematical model of the system, classical analytical approaches can be developed. When the complexity of the system implies multiphysics, the use of a method in which the subsystems communicate by exchanging a universal physics quantity, like energy, can facilitate the construction of the system's mathematical model. This potential is brought by bond graphs, and when modeling spatial multibody systems, by multibond graphs [1].

In this context, it may be needed to catch the dynamic behavior contribution of the joints between bodies of the system and therefore to characterize the stiffness and damping of the links between the bodies. Tiernego and Bos [1] introduced a systematic method to model mechanical systems with multibond graphs. In [2], Zeid proposed a library of joints and their respective equivalents in bond graphs that satisfy the classic constraint equations of each joint. In [3], he also proposed and demonstrated how to obtain an explicit formulation of the constraint equations by developing a singularly perturbed formulation for bond graphs. The result basically consists in adding R and C elements to the common flow junctions representing each degree of freedom of a joint. He also points out the fact that tuning the values of these elements can be useful to obtain an explicit formulation of the equations of motion and that other linear or nonlinear characteristics of the joints can also be obtained by working on the expression of these elements. In [4], a non-extensive translation of the library from scalar to vector bond graphs can be found.

Modeling rotating bodies around more than two non co-linear directions is trickier than translating bodies, especially due to the non-obvious trajectories and the nonlinear gyroscopic effects that appear in the equations of motion. When three translational degrees of freedom between two bodies need to be constrained, a spherical joint or three concatenated revolute joints can be used to constraint the movements, see Fig. 1.

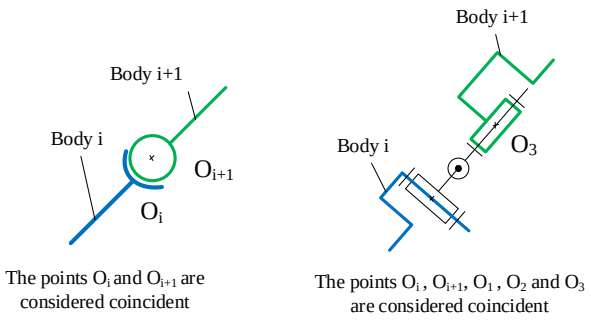

Fig. 1. Spherical joint and three concatenated revolute joints

The first section details, more explicitly than what can be found in literature, the rotation axes around which the dissipative or/and capacitive elements addition play a role; in the second section, a multibond graph joint architecture

is proposed to model stiffness and damping around three rotational degrees of freedom combining literature's spherical and revolute joints formulations. To illustrate the proposal, an inertial navigation system is modeled and simulated in the last section. Future work will show how this method can be extended to more complex systems such as rotorcraft blades' connections with its rotor hub.

II. MODELING STIFFNESS AND DAMPING WITH THREE ROTATIONAL DEGREES OF FREEDOM

The two main classic approaches to obtain the equations of motion of mechanical systems are Newton-Euler and Lagrange. In [1], Tiernego and Bos describe the multibond graph procedure using a Newton-Euler description of the system. In [5], Karnopp describes the bond graphs from a Lagrange point of view. Obviously, the two procedures give the same result; but in terms of resulting graph visibility, when modeling large systems, the Newton-Euler approach bond graph result is the one that keeps closer to the physical system – the results presented concern this approach. Again, for a visibility concern, Euler angles are used in this work; but the logic deployed can be extended to another set of Euler angles or more generally to quaternions. Concerning the representation of three degrees of freedom between two rigid bodies, Fig. 2 shows an equivalent of Fig. 1, using multibond graphs based on [2] and [4].

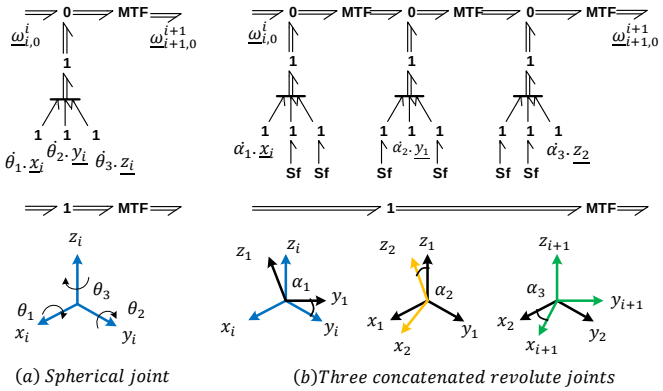

Fig. 2. Angular velocities axis in multibond graphs

Since neither R nor C elements have been added, and taking into account that the flow sources are null, the joints represented are ideal joints. In Fig. 2, the details of the angular velocities show how the multibond graphs architectures of the joints constraint the axes around which R or C elements can be added. In the spherical joint, these elements can only be added around body *i* reference frame axes while the concatenation of three revolute joints permits to add them around intermediary reference frames axes. Obviously, the choice of one or another joint solution depends on the modeling. However, it is important to distinguish the bond graph architecture of a joint and the coordinates that can be chosen to observe the relative motion between bodies *i* and *i+1*.

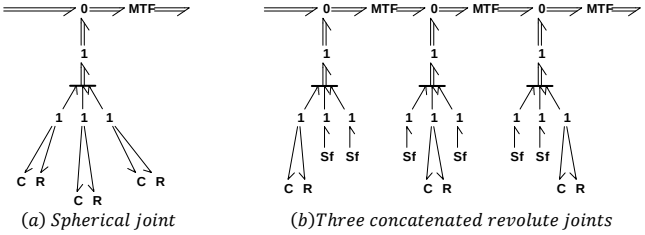

Fig. 3. Adding stiffness and damping on each degree of freedom

By adding stiffness and damping characteristics in both solutions we obtain Fig. 3. Even if for both joints, the relative angular velocity vector between body *i+1* and the inertial reference frame R_0 are equal, the dissipative and capacitive bond graph elements are not placed exactly around the exact same axes.

Causality analysis

If we now add the causal layer to the graphs, the use of null flow sources to block the degrees of freedom of a joint in a multibond graph imposes the causality of the 1 junction in red circles and ellipse on Fig. 4. In the case of the spherical joint, the two possible causalities may be assigned when for the three revolute joints only one can be assigned.

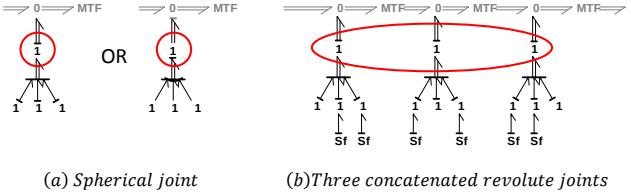

Fig. 4. Causality restrictions

As a result, for the three concatenated revolute joints, only two causality assignments are possible for the common effort (zero) junction above the common flow (one) junctions mentioned before. This limits the number of available modeling hypothesis for the rest of the multibond graph. The "blocked degrees of freedom" will have to be modeled with very low values of C elements (high stiffness) or, the inertial elements of a rigid body multibond graph will have a derivative causality. From a mathematical stand point, derivative causalities mean the system is described by differential algebraic equations (DAE). Depending on the index of the DAE, an adapted solver might still be able to simulate the system.

On the other hand, for the spherical joint, the causality of the common effort (zero) junction still has three possibilities.

The conclusion is that the multibond graph architecture of the spherical joint has a more relaxed causality. Relaxing the causal constraints results useful when modeling large spatial mechanical systems since it allows limiting the number of inertial elements with derivative causalities in rigid bodies' multibond graphs.

If we now want to keep the reduced causality constraints of the spherical joint bond graph architecture but still be able to add some stiffness and damping around the axes just

like with three revolute joints, how could we do? This issue is addressed in the next paragraph, and a new multibond graph joint architecture physically equivalent to three concatenated revolute joints is proposed.

III. PROPOSING A MULTIBOND GRAPH FOR MODELING THREE ROTATIONAL DEGREES OF FREEDOM

The idea is to simplify multiple revolute joints bond graph architectures in order to release the causal constraint while being able to add stiffness and damping around the intermediate axes between bodies *i* and *i+1* – Fig. 5.

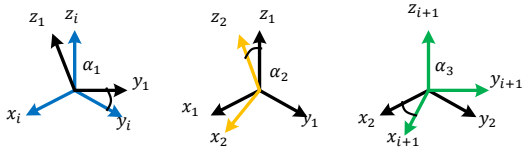

Fig. 5. Intermediate reference frames definitions

The result is presented in Fig. 6. The next paragraphs discuss its mathematical foundations.

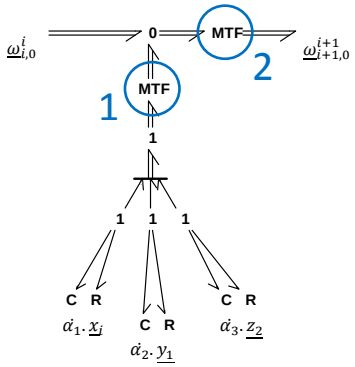

Fig. 6. Multibond graph proposal to represent three concatenated revolute joints

Mathematical foundations

The idea is to demonstrate that for both three revolute joints and the new architecture proposed the expression of $\underline{\omega}^{i+1}_{i+1,0}$ is equivalent. As demonstrated by Tienergo and Bos in [1], the demonstration for efforts follows the same steps as for flows. Therefore, it will not be presented. It is assumed that $\underline{\omega}^{i}_{i,0} = 0$, but it could also be proven when this quantity is not null. Starting with the three revolute joint, see Fig. 7,

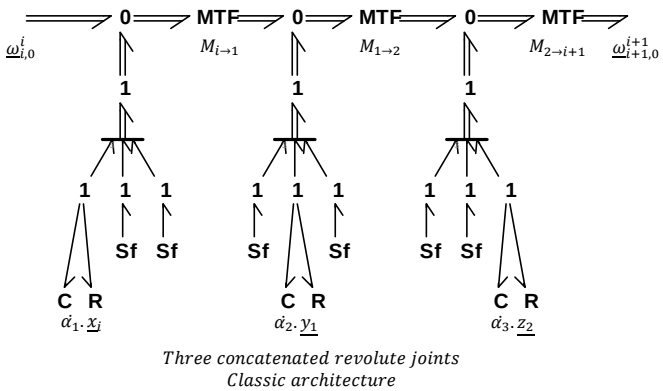

Fig. 7. Intermediate reference frames definitions

Based on basic bond graph rules applied to Fig. 7, it can be demonstrated that,

$$\underline{\omega}^{i+1}_{i+1,0} = M_{2\to i+1}\left[M_{1\to2}\left[M_{i\to1}\left[\underline{\omega}^{i}_{i,0} + \dot{\alpha}_1\begin{pmatrix}1\\0\\0\end{pmatrix}\right] + \dot{\alpha}_2\begin{pmatrix}0\\1\\0\end{pmatrix}\right] + \dot{\alpha}_3\begin{pmatrix}0\\0\\1\end{pmatrix}\right] \quad (1)$$

Where,

$$\mathrm{M_{i\to1}} = \begin{bmatrix}1 & 0 & 0\\ 0 & \cos\alpha_1 & -\sin\alpha_1\\ 0 & \sin\alpha_1 & \cos\alpha_1\end{bmatrix}^t \quad (2)$$

$$\mathrm{M_{1\to2}} = \begin{bmatrix}\cos\alpha_2 & 0 & \sin\alpha_2\\ 0 & 1 & 0\\ -\sin\alpha_2 & 0 & \cos\alpha_2\end{bmatrix}^t \quad (3)$$

$$\mathrm{M_{2\to i+1}} = \begin{bmatrix}\cos\alpha_3 & -\sin\alpha_3 & 0\\ \sin\alpha_3 & \cos\alpha_3 & 0\\ 0 & 0 & 1\end{bmatrix}^t \quad (4)$$

The development of (1) gives,

$$\underline{\omega}^{i+1}_{i+1,0} = \begin{pmatrix}\cos\alpha_3.\cos\alpha_2.\dot{\alpha}_1 + \sin\alpha_3.\dot{\alpha}_2\\ -\cos\alpha_2.\sin\alpha_3.\dot{\alpha}_1 + \cos\alpha_3.\dot{\alpha}_2\\ \sin\alpha_2.\dot{\alpha}_1 + \dot{\alpha}_3\end{pmatrix} \quad (5)$$

Now, in the case of the new architecture proposal, we defined,

$$\underline{\omega}_{i+1,i} = \dot{\alpha}_1.\underline{x}_i + \dot{\alpha}_2.\underline{y}_1 + \dot{\alpha}_3.\underline{z}_2 \quad (6)$$

As a result, $\underline{\omega}^{i}_{i+1,i}$ can be expressed by,

$$\underline{\omega}^{i}_{i+1,i} = \mathrm{M_{jacobian}}.\begin{pmatrix}\dot{\alpha}_1\\ \dot{\alpha}_2\\ \dot{\alpha}_3\end{pmatrix} \quad (7)$$

Where,

$$\mathrm{M_{jacobian}} = \begin{bmatrix}1 & 0 & \sin\alpha_2\\ 0 & \cos\alpha_1 & -\cos\alpha_2\sin\alpha_1\\ 0 & \sin\alpha_1 & \cos\alpha_1\cos\alpha_2\end{bmatrix} \quad (8)$$

And since basic bond graph rules applied to Fig. 6 give,

$$\underline{\omega}^{i+1}_{i+1,0} = \mathrm{M_{i\to i+1}}.\left(\underline{\omega}^{i}_{i,0} + \underline{\omega}^{i}_{i+1,i}\right) \quad (9)$$

Where,

$$\mathrm{M_{i\to i+1}} = (\mathrm{M_{1\to i}}.\mathrm{M_{2\to1}}.\mathrm{M_{i+1\to2}})^t \quad (10)$$

The development of (9) finally gives,

$$\underline{\omega}^{i+1}_{i+1,0} = \begin{pmatrix}\cos\alpha_3.\cos\alpha_2.\dot{\alpha}_1 + \sin\alpha_3.\dot{\alpha}_2\\ -\cos\alpha_2.\sin\alpha_3.\dot{\alpha}_1 + \cos\alpha_3.\dot{\alpha}_2\\ \sin\alpha_2.\dot{\alpha}_1 + \dot{\alpha}_3\end{pmatrix} \quad (11)$$

Equation (11) is equal to (5). As a result, the MBG architecture proposed is equivalent to literature's three concatenated revolute joints architecture by modulating its first transformer element by $\mathrm{M_{jacobian}}$ and its second transformer by $\mathrm{M_{i\to i+1}}$ (see Fig. 6).

IV. APPLICATION TO AN INERTIAL NAVIGATION SYSTEM

In order to illustrate the architecture proposal, the previous results are applied to an inertial navigation system. Inertial navigation systems (INS) are used in vehicles such as aircrafts and spacecrafts to implement motion control or guidance for pilots. An interesting advantage of an INS is its form of navigation that does not rely on external references [8]. To illustrate the concept, we will study the change of orientation of a rotorcraft in hover flight due to a wind gust. The principle of the INS consists in deducing the actual orientation of a rotorcraft by comparing it to a reference frame. One of the technologies to create a reference frame consists in isolating what we call a platform (see Fig. 8) from the rotorcraft: this can be achieved by concatenating three concentric gimbals linked by revolute joints.

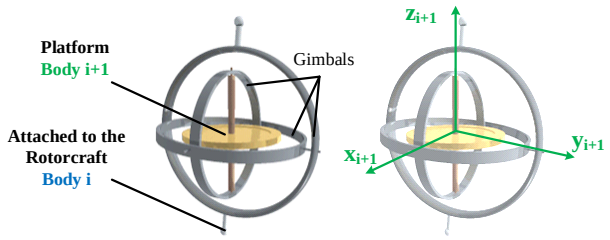

Fig. 8. Inertial navigation system

Fig. 9 describes two rigid bodies: the rotorcraft and the INS platform. Please refer to Appendix 1 to see the multibond graphs models of the complete system. The translations of the bodies have not been considered, our focus is on rotations.

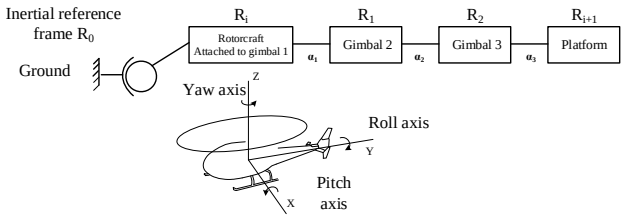

Fig. 9. Frames and parameters definitions

The objective of the INS is to be able to provide pitch, roll and yaw angles (θ_1, θ_2 and θ_3) estimations thanks to the measures of $\dot{\alpha_1}, \dot{\alpha_2}$and $\dot{\alpha_3}$. As said before, an inertial reference frame R_{i+1} can be created inside the rotorcraft, by isolating the platform. Therefore we can establish that,

$$\underline{\omega}_{i+1,0} = \underline{0} \tag{12}$$

Physically, this condition can be obtained with an adapted adjustment of the stiffness and damping between the gimbals. As a matter of fact, it can be easily imagined that the smaller the damping between the gimbals is; the less, efforts can be transmitted to the platform and therefore the easier it is, to keep the platform still.

The angular velocity of the rotorcraft can be written as,

$$\underline{\omega}_{i,0} = \underline{\omega}_{i,i+1} + \underline{\omega}_{i+1,0} \tag{13}$$

As a result, the angular rates of the rotorcraft can be determined by simply knowing the angular rates of the gimbals,

$$\underline{\omega}_{i,0} = \underline{\omega}_{i,i+1} \tag{14}$$

We can therefore express the pitch, roll and yaw angles in the reference frame created by the platform,

$$\begin{pmatrix} pitch \\ roll \\ yaw \end{pmatrix} = \int \underline{\omega}_{i,i+1}^{i+1} . dt = \int -\underline{\omega}_{i+1,i}^{i+1} . dt \tag{15}$$

Using (7), and projecting the vector in *i+1* frame,

$$\begin{pmatrix} pitch \\ roll \\ yaw \end{pmatrix} = -\int M_{i\to i+1} . M_{jacobian} . \begin{pmatrix} \dot{\alpha_1} \\ \dot{\alpha_2} \\ \dot{\alpha_3} \end{pmatrix} . dt \tag{16}$$

With $M_{i\to i+1}$ and $M_{jacobian}$ defined as in the previous section.

Equation (16) allows to estimate the pitch, roll and yaw angles by measuring the angular velocities of the INS gimbals ($\dot{\alpha_1}$, $\dot{\alpha_2}$and $\dot{\alpha_3}$).

Simulation results

In order to illustrate the new joint architecture proposed, we compare the simulation results of the system's model described in Fig. 9 and Appendix 1. The two models compared are the one with three classic concatenated revolute joints and one with the new architecture proposed – see Appendix 1. At t=1s, a wind gust modeled by a torque impulse impacts the rotorcraft on each of its axis. The idea being to perturb the rotorcraft on its pitch, roll and yaw axis we approximate the action of the wind as a torque and not a force on its fuselage.
The simulation results are presented in Fig. 10. Since we have chosen high viscous friction coefficients between the air and the fuselage, the rotorcraft motion is highly damped and the fuselage does not oscillate around an equilibrium position. Fig. 10 shows that both architectures give the same results.

In Fig. 11, we plot the orientation of the platform in the inertial reference frame and define these angles as β_1,β_2 and β_3. It can be observed in Fig. 11 that the three angles deviate from zero. This can be expected since the platform was not ideally isolated (see the dissipative and capacitive values for the platform isolation in Appendix 1). Another INS technology could be considered to maintain (12) to a desired approximation [8].

What we are interested in illustrating in Fig. 10 and Fig. 11 is that the proposed multibond graph converges with the classic three concatenated revolute joints.

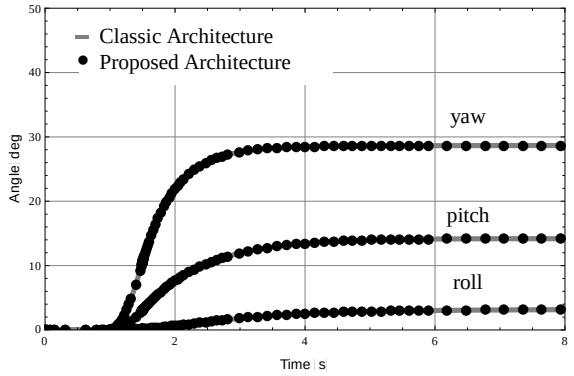

Fig. 10. Rotorcraft orientation comparison using the two MBG architectures

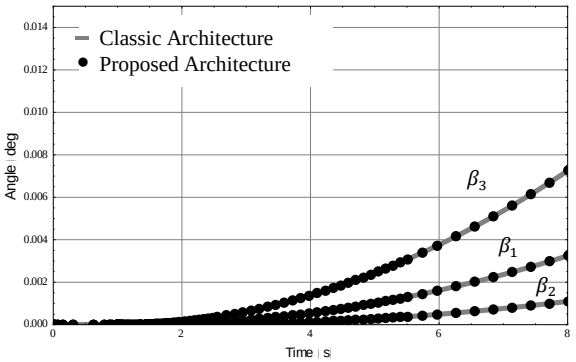

Fig. 11. Platform orientation deviation comparison using the two MBG architectures

Causality analysis of the models

In Appendix 1, in Fig. 12, the inertial element that characterizes the platform is in derivative causality as discussed in the section II. This is the case whether the ground is modeled as a stiff capacitive element or a null source of flow.

On the other hand, the model that contains the new architecture proposal in Fig. 13 can keep its integral causality even if the null flow source is introduced. Keeping an integral causality is also an advantage since the mathematical model of the system is a set of Ordinary Differential Equations (ODEs), which enables a systematic numerical resolution of the ODEs [9].

V. CONCLUSION AND FUTURE WORK

This paper illustrates the different ways of modeling stiffness and damping using multibond graphs when two bodies of a mechanical system are constrained by three rotational degrees of freedom. It highlights where dissipative and capacitive bond graph elements need to be added depending on modeling hypotheses.

A multibond graph architecture simplification for the concatenation of three revolute joints is proposed; and illustrated through the example of an inertial navigation system. The potential of this architecture simplification in the limitation of derivative causalities has also been demonstrated. This can be particularly useful when modeling larger mechanical systems.

Future work could include Euler parameters or quaternions instead of Euler angles in order to avoid any mathematical singularities such as the famous gimbal lock of the inertial navigation system in Apollo 11. It will also be shown how this method can be extended to more complex systems such as rotorcraft blades' connections with its rotor hub.

ACKNOWLEDGMENTS

This work was supported by the “Complex Mechanical Systems Dynamics” project - EADS Foundation - Arts et Metiers Paristech.

REFERENCES

[1] M.J.L. Tiernego, A.M. Bos, *Modelling the dynamics and kinematics of mechanical systems with multibond graphs*, Journal of the Franklin Institute, Volume 319, Issues 1–2, January–February 1985

[2] Ashaf Zeid, Chih-Hung Chung, *Bond graph modeling of multibody systems: a library of three-dimensional joints*, Journal of the Franklin Institute, Volume 329, Issue 4, July 1992

[3] Ashaf Zeid, James Overholt, *Singularly Perturbed Formulation: Explicit Modeling of Multibody System*, Journal of the Franklin Institute, 1995

[4] Wolfgang Borutzky, Bond Graph Methodology, Development and Analysis of Multidisciplinary Dynamic System Models, 2010

[5] Karnopp,D.C., *Lagrange's equations for complex bond graph systems*, Journal of Dynamic Systems, Measurement and Control, 1977

[6] P.E. Nikravesh, I.S.Chung, Application of Euler Parameters to the Dynamic Analysis of Three-Dimensional Constrained Mechanical Systems, Journal of Mechanical Design, ASME, 1982

[7] Wilfrid Favre, Serge Scavarda, *Bond graph representation of multibody systems with kinematic loops*, Journal of the Franklin Institute, Volume 335, Issue 4, May 1998

[8] Stieler B., Winter H., *Gyroscopic Instruments and their application to flight testing*, AGARD Flight Test instrumentation series, Volume 15, NATO report, 1982

[9] Van Dijk J., Breedveld P.C., *Simulation of System Models Containing Zero-order Causal Paths*, Journal of the Franklin Institute, 1991

APPENDIX 1

(Presented next page)

APPENDIX 1

TABLE I. MODELS' DATA

Viscous friction air/fuselage	$R=10^3$ Nm.s/rad
Wind gust	Torque on each axis of R_i, Tx_i=5000 Nm Ty_i=1000 Nm Tz_i=10000 Nm
Platform isolation	$C=10^{-5}$Nm/rad $R=10^{-5}$ Nm.s/rad
Rotorcraft fuselage	Ixx=10 000 m².kg, Iyy=10 000 m².kg, Izz=5000 m².kg
Platform	Ixx=10 m².kg, Iyy=10 m².kg, Izz=10 m².kg

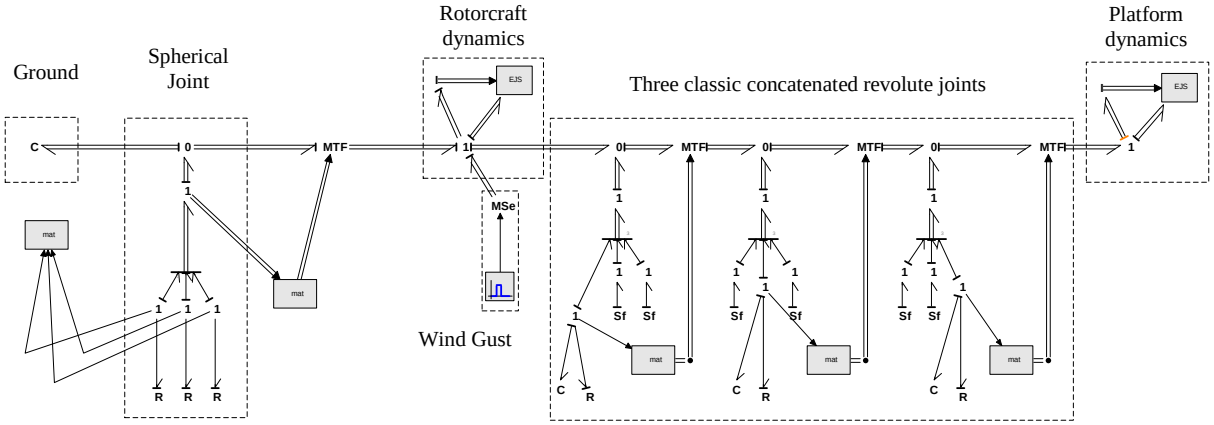

Fig. 12. Rotorcraft an INS constrained by three classic MBG concatenated revolute joints

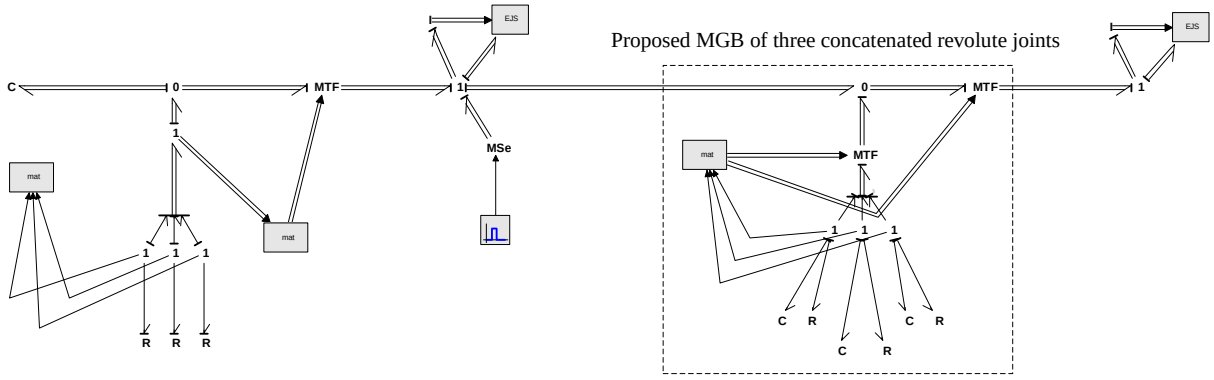

Fig. 13. Rotorcraft an INS constrained by the proposed MBG of three concatenated revolute joints